Global Research journal of Natural Science and Technology (Grjnst)
Volume: 04 - Issue 1 (2026)
p.ISSN: 2790-7643e.ISSN: 2790-7651

Magnetic Palm Kernel Shell Biochar as an Efficient Adsorbent for Organic Pollutants

Zahid H Shar

Dr. M.A. Kazi Institute of Chemistry, University of Sindh, Jamshoro, Pakistan

zahidshar_2009@yahoo.com

Eidal Khan

Government degree college Malir Cantonment Karachi

profeidalkhanbaloch110@gmail.com

Muhammad Ashraf Bajer

Government degree college Islam Kot, Thar parker

ashrafjiandani@gmail.com

Muhammad Kashif Channa

Institute of chemistry, Shah Abdul Latif University Khairpur

mkchanna18@gmail.com

Waqas Khan

Dr. M.A. Kazi Institute of Chemistry, University of Sindh, Jamshoro, Pakistan

waqas.khan202029@gmail.com

Qadeer Khan Pahanwar

Dr. M.A. Kazi Institute of Chemistry, University of Sindh, Jamshoro, Pakistan

qadeer.panhwar@usindh.edu.pk

DOI: https://doi.org/10.53762/grjnst.04.01.02

Abstract: *Water contamination by organic pollutants is a serious hazard to human health. In order to remove salicylic acid (SA) and 4-nitroaniline (4-NA) from aqueous solutions, this work developed magnetically recoverable biochar from palm kernel shell using a co-precipitation approach. Scanning electron microscopy (SEM) and Fourier transform infrared (FTIR) spectroscopy were used to analyze the synthesized magnetic biochar, revealing its porous structure and successful magnetization with Fe_3O_4 particles. For both pollutants, the MBC showed high removal efficiencies—above 90% under ideal circumstances. The Langmuir isotherm model yielded maximal adsorption capacities of 144 mg/g for 4-NA and 155 mg/g for SA. The equilibrium data were best explained by the Langmuir isotherm, indicating monolayer adsorption on a homogeneous surface. Additionally, the study showed that adsorption was strongly pH-dependent, with 4-NA being best removed at a pH that was almost neutral. The biochar's magnetic characteristic made it simple to separate it from treated water using an external magnet. These results suggest that magnetic palm kernel shell biochar is a possible substitute for traditional activated carbon as a highly efficient, inexpensive, and readily separable adsorbent for treating water contaminated with developing organic contaminants.*

Keywords: *Magnetic biochar; Adsorption; Salicylic acid; 4-Nitroaniline; Water treatment; Langmuir isotherm; Palm kernel shell.*

1. Introduction

Discharges from industrial, agricultural, and residential sources continue to be the leading cause of organic pollutant water contamination worldwide (Morin-Crini, Lichtfouse et al. 2022, Sharma, Rajan et al. 2024). Because of their toxicity, stability, and propensity for bioaccumulation, persistent organic pollutants (POPs) and new contaminants including pharmaceutical active chemicals (PhACs) and industrial intermediates are especially concerning (Boethling, Fenner et al. 2009, Akhtar, Naseem et al. 2021). Two such substances that are commonly found in wastewater effluents and surface waters are salicylic acid (SA), a main metabolite of aspirin (acetylsalicylic acid), and 4-nitroaniline (4-NA), a precursor in dye, insecticide, and pharmaceutical manufacture (Karunanayake 2017). Given that Salicylic Acid has demonstrated xenobiotic estrogenic effects and 4-Nitroaniline is categorized as a possible carcinogen, their cumulative presence warrants careful monitoring to mitigate risks to public health and aquatic life (Zhang, Jia et al. 2012, Bernauer, Bodin et al. 2023). Therefore, it is essential to create sustainable and effective technology for their elimination.

Organic pollutants have been removed using a variety of treatment techniques, such as membrane filtration, coagulation, sophisticated oxidation processes, and adsorption (Hanafi and

Sapawe 2020, Thirunavukkarasu, Nithya et al. 2020). Because of its ease of use, affordability, and efficiency, adsorption is frequently preferred, particularly when employing porous adsorbents (Akhtar, Ali et al. 2024). The most used adsorbent, activated carbon (AC), has drawbacks, including high production costs and challenging recovery and separation from treated water (Shah, Amin et al. 2025). A possible, affordable substitute for AC is biochar, a carbon-rich substance made by pyrolyzing biomass in an oxygen-limited environment (Sajjadi, Zubatiuk et al. 2019). The adsorption of different pollutants is facilitated by its porous structure and surface functional groups, such as -OH and -COOH (Zeng, Tan et al. 2022).

However, conventional biochar's fine powder form makes it more difficult to separate after usage, which could result in secondary contamination. In order to get around this, iron oxides (such as Fe_3O_4) are added to biochar to magnetize it. This results in a composite material called magnetic biochar, or MBC, which combines the adsorption capacity of biochar with the magnetic separability of iron oxides (Reddy and Lee 2014, Singh, Pant et al. 2023). This increases the material's suitability for water treatment applications by enabling quick and effective recovery utilizing an external magnet.

This investigation employed a co-precipitation method to synthesize magnetic biochar from palm kernel shell (PKS), an abundant agricultural waste. The research objectives encompassed the synthesis and characterization of the magnetic biochar composite using Scanning Electron Microscopy (SEM) and Fourier Transform Infrared (FTIR) spectroscopy, evaluation of its adsorptive capacity for removing salicylic acid (SA) and 4-nitroaniline (4-NA) from aqueous solutions, systematic investigation of key operational parameters including adsorbent dosage, solution pH, and initial pollutant concentration, and elucidation of adsorption mechanisms through Langmuir and Freundlich isotherm modeling. This study provides a comprehensive assessment of magnetic biochar as a sustainable and magnetically recoverable adsorbent for mitigating SA and 4-NA contamination in aquatic systems.

2. Materials and Methods

2.1. Materials

Palm kernel shell (PKS) biochar was obtained from the Indus Biochar, Karachi**.** Ferric chloride ($FeCl_3$), ferrous sulfate heptahydrate ($FeSO_4 \cdot 7H_2O$), sodium hydroxide (NaOH), salicylic acid (SA, $C_7H_6O_3$), and 4-nitroaniline (4-NA, $C_6H_6N_2O_2$) of analytical grade were purchased from R&M Chemical Company and used without further purification. All solutions were prepared using distilled water.

2.2. Synthesis of Magnetic Biochar (MBC)

The MBC was synthesized following a modified co-precipitation method (Reddy and Lee 2014). Briefly, 100 g of PKS biochar was ground, sieved to a particle size of 0.1–0.6 mm, and 50 g of this fraction was dispersed in 500 mL of distilled water. Separately, an iron solution was prepared by dissolving 18.0 g of $FeCl_3$ in 1300 mL of distilled water at 60°C, followed by the addition of a solution containing 36.6 g of $FeSO_4 \cdot 7H_2O$ in 150 mL water. The iron solution was then vigorously mixed for 5 minutes. The biochar suspension was added to this iron solution, and the mixture was stirred slowly at room temperature for 30 minutes. The pH of the suspension was adjusted to 10–11 using 10 M NaOH, resulting in a color change to black, indicating the precipitation of magnetic iron oxides. The mixture was stirred for an additional hour and then aged for 24 hours. The resulting MBC was collected via vacuum filtration, washed repeatedly with distilled water and ethanol, and dried in an oven at 50°C for 48 hours.

2.3. Characterization

Adsorption is driven by the surface shape and functional groups that are present on any material's surface. FTIR and SEM spectra were gathered in order to comprehend the mechanism of SA and 4-NA adsorption on the MBC surface. FT-IR (Thermo Nicolet) with a ZnSe crystal under OMNIC software control was used to record IR spectra. Using a scanning electron microscope (Zeiss, JEOL-JSM-35CF, UK) operating at invariable pressure (VP) mode at 0.3 tor and 20 kV accelerating voltage, surface morphology and structure were ascertained. 5 kV was used to record SEM spectra.

2.4. Batch Adsorption Experiments

SA and 4-NA stock solutions (25 ppm each) were made in distilled water. 40 mL glass vials with 25 mL of pollutant solution were used for batch tests. Different masses of MBC (0.005–0.100 g) were added to solutions containing a mixture of SA and 4-NA (25 ppm each) in order to investigate the impact of adsorbent dose. To guarantee mixing, the vials were vortexed for two to three minutes. A portable magnet was then used to separate the MBC and adsorbed contaminants. The concentration of remaining pollutants in the clear supernatant was measured. Similarly, by keeping the concentration fixed at 50 mg/L and adsorbent dose (0.05 g) the impact of pH (2–11) was investigated. The pH was varied using 0.1 M HCl or NaOH. The effect of initial concentration (100–300 ppm) was also investigated. All experiments were performed at room temperature (25 ± 2°C).

2.5. Analytical Methods and Calculations

The concentrations of SA and 4-NA before and after adsorption were determined using a UV-Visible spectrophotometer. SA was quantified at its maximum absorbance wavelength (λ_max = 298

nm) and 4-NA at λ_max = 378 nm. Calibration curves ($R^2 > 0.99$) were constructed using standard solutions. The amount of pollutant adsorbed at equilibrium, q_e (mg/g), was calculated using Eq. (1):

$$q_e = \frac{(C_0 - C_e)V}{M} \qquad \text{Eq.……1}$$

where C_0 and C_e are the initial and equilibrium concentrations (mg/L), respectively, V is the solution volume (L), and M is the mass of MBC (g).

The removal efficiency (%) was calculated using Eq. (2):

$$\%Removal = \frac{(C_0 - C_e)}{C_0} \times 100 \qquad \text{Eq.……2}$$

2.6. Adsorption Isotherms

Equilibrium adsorption data were analyzed using Langmuir (Eq. 3) and Freundlich (Eq. 4) isotherm models.

$$\frac{C_e}{q_e} = \frac{1}{K_L q_m} + \frac{C_e}{q_m} \text{(Langmuir)} \qquad \text{Eq.……3}$$

$$\log q_e = \log K_F + \frac{1}{n} \log C_e \text{(Freundlich)} \quad \text{Eq.……..4}$$

where q_m is the maximum monolayer adsorption capacity (mg/g), K_L is the Langmuir constant related to adsorption energy (L/mg), and K_F and n are Freundlich constants related to adsorption capacity and intensity, respectively.

3. Results and Discussion

3.1. Characterization of MBC

The MBC had a macro-porous and heterogeneous surface structure with pore diameters ranging from 1 to 5 µm, according to the SEM image (Figure 1). The adsorption of organic molecules is facilitated by this porous shape and large surface area (Jaafar, Clode et al. 2015). The efficient deposition and dispersion of Fe_3O_4 nanoparticles, which were essential for the magnetic response, was demonstrated by the presence of brilliant, granular clusters on the surface.

Figure 1: SEM image of magnetic biochar

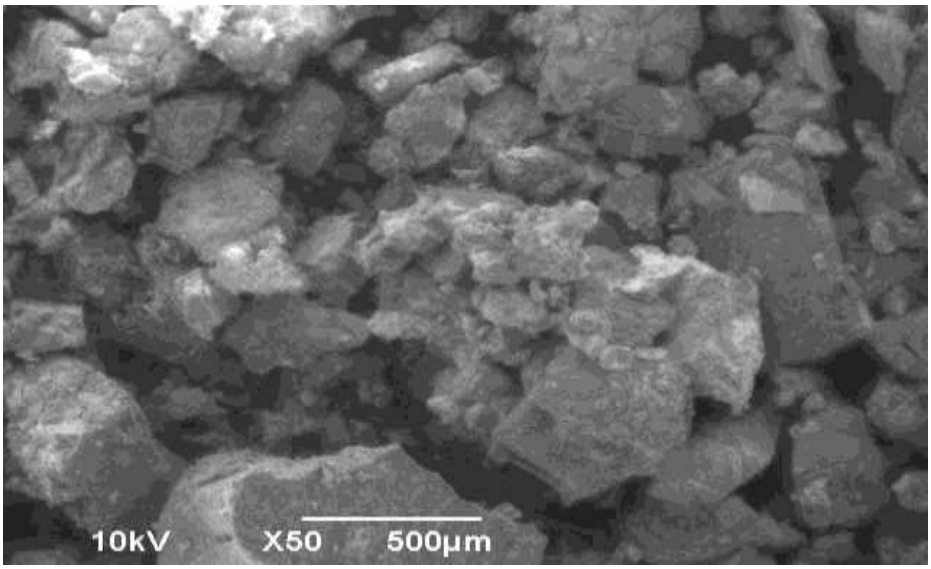

Figure 2: FTIR spectrum of MBC

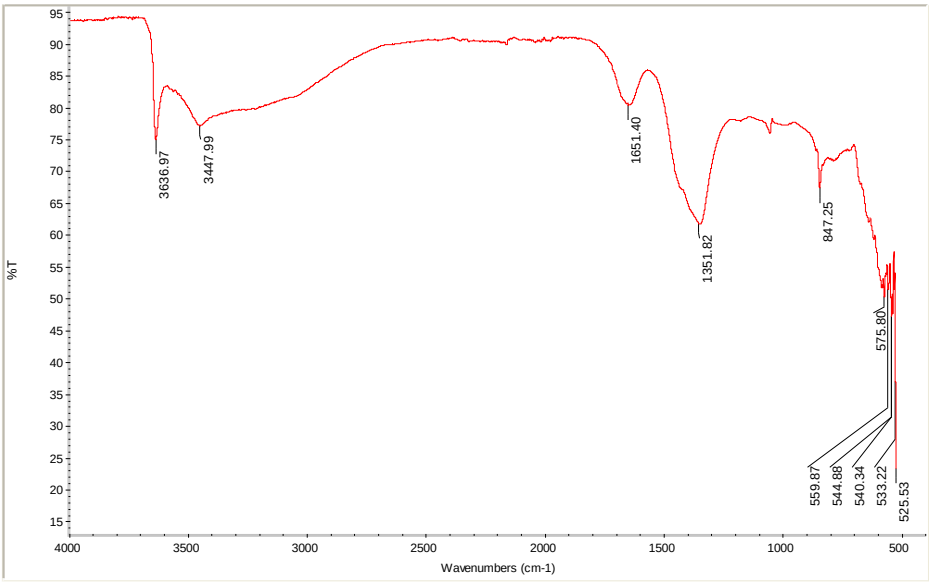

Important functional groups on the MBC surface were detected by the FTIR spectrum (Figure 2). O-H stretching vibrations of hydroxyl groups were identified as the cause of the broad peak at 3409 cm^{-1}. Alkyl C-H stretching was represented by peaks at 2977 and 2920 cm^{-1}. Peaks at 1159 and 1069 cm^{-1} were attributed to C-O-C stretching vibrations, while the band at 1580 cm^{-1} showed the existence of carboxylate (COO^-) groups. The peaks in the 942–679 cm^{-1} range were caused by C–H bond deformation modes. Through processes including hydrogen bonding and electrostatic attraction, these functional groups—especially -OH and -COOH—play a crucial part in interacting with organic contaminants (Yang and Yuan 2025). The spectrum verified that the magnetization process created Fe-O bonds (indicated by peaks below 600 cm^{-1}, not shown in full range), enabling both adsorption and magnetic separation, rather than destroying the biochar's functional groups.

3.2. Effect of Operational Parameters

3.2.1. Effect of Adsorbent Dosage

When the MBC dosage was increased from 0.005 to 0.100 g, the elimination efficiency of both SA and 4-NA rose significantly (Figure 3). This pattern is anticipated as a greater dosage increases the surface area and accessible adsorption sites (Zheng, Lv et al. 2023). The removal efficiency for 4-NA rose from 46.72% (0.005 g) to 97.28% (0.100 g). In a similar way, elimination rose from 28.00% to 92.32% for SA. At higher dosages (>0.05 g), the incremental increase in removal efficiency decreased, most likely as a result of particle aggregation or active site overlap that decreased the effective surface area (Mashoene 2022).

3.2.2. Effect of Solution pH

Solution pH is a critical factor influencing adsorption, as it affects both the surface charge of the adsorbent and the ionization state of the pollutant. The adsorption of 4-NA onto MBC was highly pH-dependent (Figure 4). Maximum removal was observed at pH 4 and pH 7, with a sharp decrease in adsorption at highly alkaline conditions (pH > 10). 4-NA exists primarily in its neutral molecular form in the studied pH range. The MBC surface is expected to be positively charged at lower pH (pH < pzc) and negatively charged at higher pH. Maximum adsorption at pH 4–7 stems from strong pi-pi interactions, hydrogen bonding, and electron donor-acceptor mechanisms. The decline at alkaline pH is likely due to increased electrostatic repulsion between the negatively charged MBC surface and competing ions or the deprotonated adsorbate

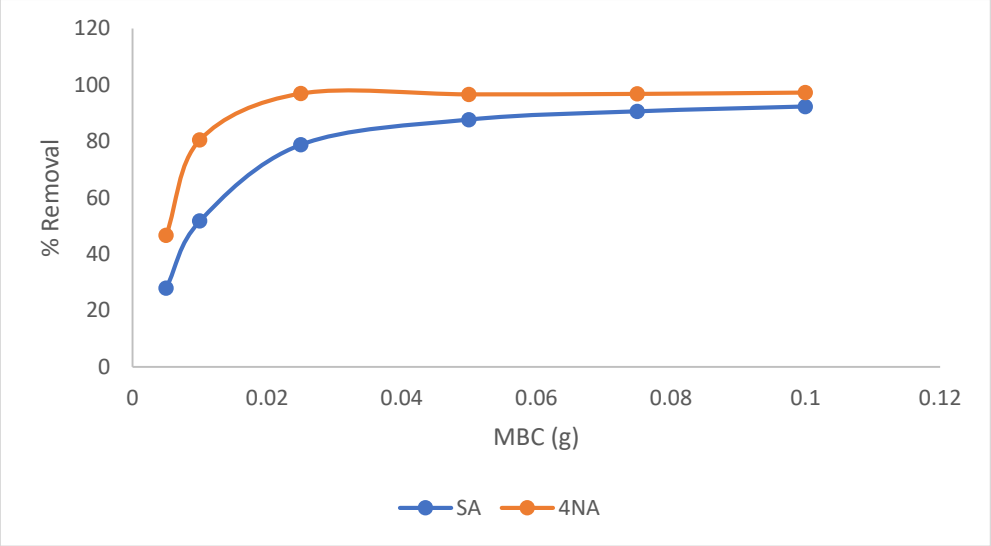

Figure 3: % Removal vs. MBC mass for SA and 4-NA

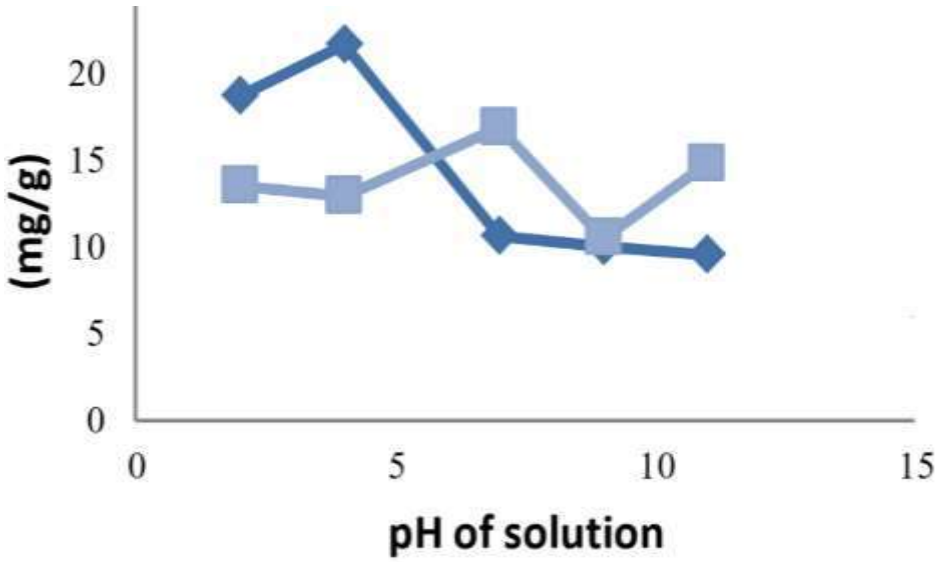

Figure 4: Effect of pH on 4-NA adsorption

3.2.3. Effect of Initial Concentration and Contact Time

As the initial concentration of 4-NA increased from 100 to 300 mg/L (at fixed adsorbent dose), the amount adsorbed per unit mass (q_e) increased, while the percentage removal decreased (Figure 5). This is because, at a fixed adsorbent dose, the number of available active sites is constant. At lower concentrations, sites are in excess, leading to high percentage removal. At higher concentrations, sites become saturated, increasing the absolute amount adsorbed (q_e) but lowering the removal efficiency. Similar trends were observed for SA. Equilibrium was reached within approximately 60 minutes for both pollutants, indicating rapid adsorption kinetics.

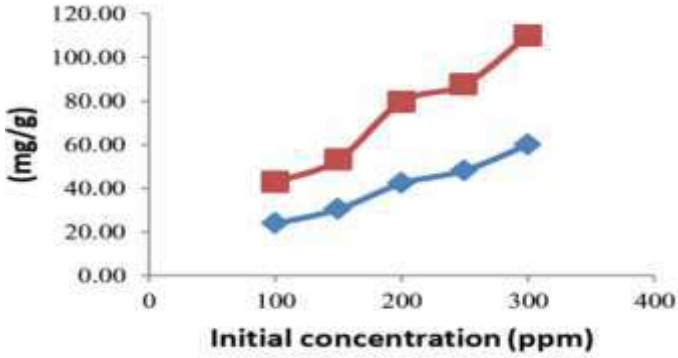

Figure 5: Effect of initial concentration on adsorption

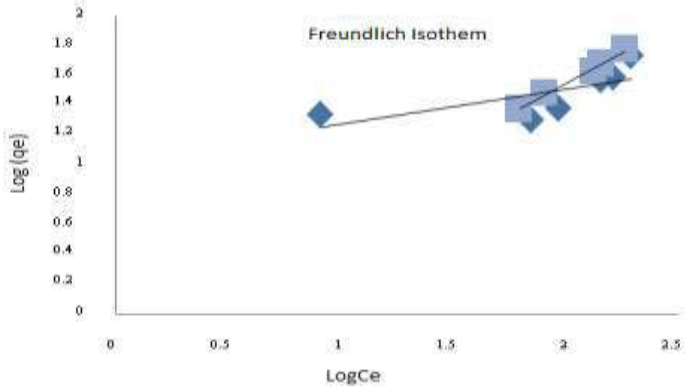

Figure 6: Langmuir isotherm plot

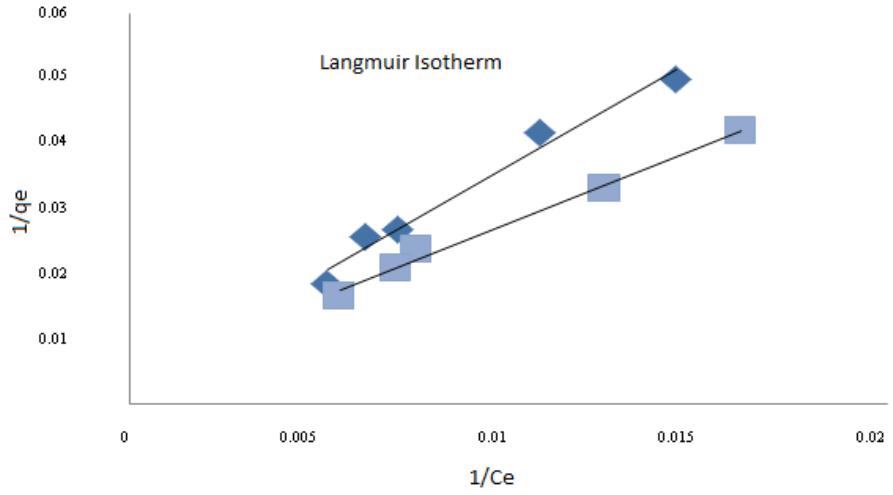

Figure 7: Freundlich isotherm plot

3.3. Adsorption Isotherms

The equilibrium adsorption data for SA and 4-NA were fitted to Langmuir and Freundlich isotherm models (Figure 6 & 7). The calculated parameters are presented in Table 1.

Table 1: Parameters of Langmuir and Freundlich isotherm models for SA and 4-NA

		Langmuir			Freundlich	
Adsorbent	q_{max} (mg/g)	K_L	R^2	K_F	n	R^2
SA	155	0.00099117	0.98	11.15	4.31	0.48
4-NA	144	0.00204011	0.99	0.76	1.20	0.99

The Langmuir model provided an excellent fit for both pollutants, with correlation coefficients (R^2) of 0.981 and 0.990 for SA and 4-NA, respectively. This suggests that adsorption occurs via monolayer coverage on a homogeneous surface with finite identical sites (Ng, Burhan et al. 2017). The maximum monolayer adsorption capacities (q_m) predicted by the Langmuir model were 155 mg/g for SA and 144 mg/g for 4-NA. These values are comparatively high, underscoring the effectiveness of the synthesized

MBC. The Freundlich model fitted well for 4-NA (R^2=0.99, n>1) but poorly for SA (R^2=0.484), indicating that the adsorption of 4-NA might also have a component of multilayer adsorption on a heterogeneous surface, while SA adsorption is predominantly monolayer. The 'n' value for 4-NA (1.20) indicates favorable adsorption. Langmuir maximum adsorption capacities (q_m) obtained in this study 155 mg/g for SA and 144 mg/g for 4-NA—are notably high. This positions the PKS-derived MBC as a highly effective adsorbent when benchmarked against similar materials reported in the literature. A study by (Karunanayake, Todd et al. 2017) utilizing magnetic biochar from Douglas fir (MDFBC) reported Langmuir capacities of 109 mg/g for SA and 114 mg/g for 4-NA at pH 5 and 45°C. Our capacities are slightly higher for SA and 4-NA, respectively. This superior performance can be attributed to several factors intrinsic to the PKS feedstock and the synthesis process. Palm kernel shell is a lignocellulosic material that, upon pyrolysis and magnetization, can yield a carbon structure with a favorable pore network and surface chemistry. The SEM analysis confirmed a macro-porous structure (1-5 µm), which facilitates the diffusion and accommodation of pollutant molecules. Furthermore, the distinct surface functional groups identified via FTIR, particularly the abundant -OH and -COOH groups, provide ample sites for specific interactions like hydrogen bonding and complexation, enhancing the overall uptake.

4. Conclusion

This study successfully demonstrated the synthesis of a novel magnetic biochar from palm kernel shells and its application as an efficient adsorbent for removing salicylic acid and 4-nitroaniline from water. The MBC exhibited excellent magnetic separability, a porous structure, and a functionalized surface. Under optimized conditions, it achieved removal efficiencies exceeding 90% for both pollutants. The adsorption process was best described by the Langmuir isotherm model, indicating monolayer adsorption with high maximum capacities of 155 mg/g for SA and 144 mg/g for 4-NA. The adsorption was influenced by solution pH, with optimal performance in the near-neutral range for 4-NA. The primary mechanisms involved include π-π interactions, hydrogen bonding, and pore filling. Given its high efficiency, ease of synthesis from waste biomass, and convenient magnetic recovery, MBC presents a sustainable, cost-effective, and practical solution for the remediation of water contaminated with emerging organic pollutants. Future work should focus on column studies for continuous flow systems, investigation of regeneration and reusability of MBC, and testing its efficacy on real industrial wastewater.

Acknowledgements

The authors gratefully acknowledge the laboratory support provided by the Dr. M.A. Kazi Institute of Chemistry, University of Sindh, Jamshoro.

References

Akhtar, A. B. T., et al. (2021). Persistent organic pollutants (POPs): sources, types, impacts, and their remediation. Environmental pollution and remediation, Springer**:** 213–246.

Akhtar, M. S., et al. (2024). "Innovative adsorbents for pollutant removal: exploring the latest research and applications." Molecules **29**(18): 4317.

Bernauer, U., et al. (2023). SCCS Notes of guidance for the testing of cosmetic ingredients and their safety evaluation-12th revision-Final Opinion–SCCS/1647/22-Corrigendum 2.

Boethling, R., et al. (2009). "Environmental persistence of organic pollutants: Guidance for development and review of POP risk profiles." Integrated Environmental Assessment and Management **5**(4): 539–556.

Hanafi, M. F. and N. Sapawe (2020). "A review on the current techniques and technologies of organic pollutants removal from water/wastewater." Materials Today: Proceedings **31**: A158–A165.

Jaafar, N. M., et al. (2015). "Soil microbial responses to biochars varying in particle size, surface and pore properties." Pedosphere **25**(5): 770–780.

Karunanayake, A. G., et al. (2017). "Rapid removal of salicylic acid, 4-nitroaniline, benzoic acid and phthalic acid from wastewater using magnetized fast pyrolysis biochar from waste Douglas fir." Chemical Engineering Journal **319**: 75–88.

Karunanayake, U. (2017). "Douglas Fir Biochar for Water Remediation."

Mashoene, T. N. (2022). Surface Modification of Biochar Composite Made from Tea Waste for the Removal of Selected Organic Pollutants from Aqueous Medium, Vaal University of Technology (South Africa).

Morin-Crini, N., et al. (2022). "Worldwide cases of water pollution by emerging contaminants: a review." Environmental Chemistry Letters **20**(4): 2311–2338.

Ng, K. C., et al. (2017). "A universal isotherm model to capture adsorption uptake and energy distribution of porous heterogeneous surface." Scientific Reports **7**(1): 10634.

Reddy, D. H. K. and S.-M. Lee (2014). "Magnetic biochar composite: facile synthesis, characterization, and application for heavy metal removal." Colloids and Surfaces A: Physicochemical and Engineering Aspects **454**: 96–103.

Sajjadi, B., et al. (2019). "Chemical activation of biochar for energy and environmental applications: a comprehensive review." Reviews in Chemical Engineering **35**(7): 777–815.

Shah, H. H., et al. (2025). "Overview of environmental and economic viability of activated carbons derived from waste biomass for adsorptive water treatment applications." Environmental Science and Pollution Research **32**(32): 19084–19109.

Sharma, K., et al. (2024). Water pollution: Primary sources and associated human health hazards with special emphasis on rural areas. Water resources management for rural development, Elsevier**:** 3–14.

Singh, V., et al. (2023). "Adsorption studies of Pb (II) and Cd (II) heavy metal ions from aqueous solutions using a magnetic biochar composite material." Separations **10**(7): 389.

Thirunavukkarasu, A., et al. (2020). "A review on the role of nanomaterials in the removal of organic pollutants from wastewater." Reviews in Environmental Science and Bio/Technology **19**(4): 751–778.

Yang, L. and Y. Yuan (2025). "Functional group characteristics of coal treated with clean biomass surfactant via FTIR spectroscopy." Scientific Reports **15**(1): 18676.

Zeng, W., et al. (2022). "New insights into the capture of low-level gaseous pollutants in indoor environment by carbonaceous materials: effects of functional groups, pore size, and presence of moist." Separation and Purification Technology **298**: 121652.

Zhang, Z., et al. (2012). "The estrogenic potential of salicylate esters and their possible risks in foods and cosmetics." Toxicology letters **209**(2): 146–153.

Zheng, Y., et al. (2023). "Characterization and adsorption capacity of modified biochar for sulfamethylimidine and methylene blue in water." ACS omega **8**(33): 29966–29978.